ELSEVIER

Image and Vision Computing 20 (2002) 239–248

image AND vision COMPUTING

www.elsevier.com/locate/imavis

Measuring similarity between pixel signatures

A.S. Holmes[1,*], C.J. Rose, C.J. Taylor

Imaging Science and Biomedical Engineering, University of Manchester, Stopford Building, Oxford Road, Manchester M13 9PT, UK

Received 16 October 2000; accepted 18 December 2001

Abstract

We address the problem of finding specific types of structure in medical images, such as mammograms. We use scale-orientation signatures to provide a rich description of local structure but observe that, when they are treated as vectors for statistical analysis, obvious measures of similarity such as Euclidean distance are not robust to small changes in structure. We describe three robust methods for measuring similarity, based on the transportation (earth mover's) distance. The most sophisticated of these—the *best partial matching* (BPM) distance—detects common structure between signatures, even when potentially confounding structure is also present. We compare the three new similarity measures and Euclidean distance experimentally. BPM distance is shown to give the best results for both synthetic and real mammogram data.

Keywords: Similarity measure; Scale-orientation pixel signature; Computer-aided mammography

1. Introduction

It has been shown that prompting in mammography can improve a radiologist's performance, even if the prompting system makes errors [1]. Prompting involves using computer-based image analysis to locate potential abnormalities so that the radiologist's attention can be drawn to them. One approach to detect abnormalities is to compute some form of local feature signature for each pixel and then apply a statistical classifier [2]. Recently, non-linear scale-orientation signatures have been used for the detection of malignant tumours in mammographic images [3]. The approach can, in principle, be extended to detect other normal and abnormal structures. However, when the signatures are treated as vectors for statistical classification, the Euclidean vector space they define has unsatisfactory metric properties—a small change in underlying structure may produce a large change in the vector. This provides an unsatisfactory basis for statistical analysis.

In this paper we investigate using the transportation (earth mover's) algorithm to measure the extent to which values in two signatures need to be redistributed to make them identical. This *transportation distance* is a 'natural' measure of similarity between the two signatures. We have developed unnormalised, normalised and *best partial matching* (BPM) approaches to measure the transportation distance between two signatures and compared them with Euclidean distance. Our aim is to find a measure that recognises similar structures in signatures whilst remaining robust to intrinsic variability and the presence of confounding structure.

2. Background

2.1. Non-linear scale-orientation signatures

We have previously described the construction of scale-orientation signatures using morphological filters [3]. Morphological M and N filters are known as sieves, because they remove image features (peaks or troughs) smaller than a specified size [4]. By applying 1-D sieves of increasing size to a 2-D image at a range of orientations, a scale-orientation signature can be constructed for each pixel in the image. Each signature is a 2-D array in which the columns are values for the same orientation, the rows are values for the same scale and the values themselves are the grey-level change at the pixel, resulting from the application of the sieve at a particular scale and orientation. Sieves have been shown to have desirable properties when compared to other methods of constructing scale-orientation signatures [3,5]. In particular, the results at different positions on the same structure are similar (local stationarity) and the interaction between adjacent structures is minimised.

* Corresponding author. Tel.: +44-0161-275-5130; fax: +44-0161-275-5145.

E-mail addresses: anthony.holmes@image-metrics.com (A.S. Holmes), christopher.rose@stud.man.ac.uk (C.J. Rose), chris.taylor@man.ac.uk (C.J. Taylor).

[1] Anthony Holmes is currently with Image Metrics plc.

0262-8856/02/$ - see front matter
PII: S0262-8856(02)00005-7

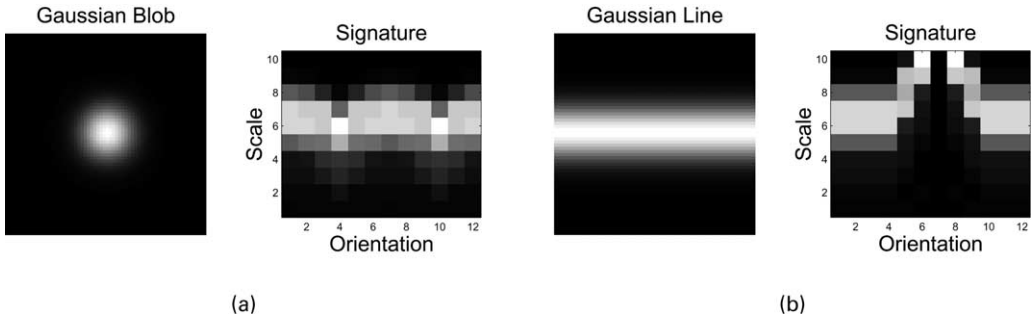

Fig. 1. Scale-orientation signatures for: (a) a Gaussian blob and (b) a Gaussian line.

Fig. 1 shows examples of scale-orientation signatures for the centre pixels of some simple structures.

2.2. Euclidean distance between signatures

Signatures can be compared or subjected to statistical analysis by forming the signature values into a vector. Euclidean distance between these signature vectors is an obvious measure of similarity, but is very sensitive to small changes in underlying structure, a small change in the scale or orientation of local structure can cause a large change in a signature vector resulting in a large change in the Euclidean distance between signatures. This is shown in Fig. 2 which shows two 1-D pixel signature vectors. Although they describe similar underlying structure, the Euclidean distance between them is large. Thus, Euclidean distance provides an unsatisfactory measure of signature similarity. A good similarity measure would be robust to small changes in scale and orientation of signature structure and, ideally, to the presence of other potentially confounding structure.

2.3. Transportation problems

Transportation problems are a class of optimisation problem in which the aim is to minimise the cost of delivering integral quantities of goods produced at n warehouses to m markets whilst balancing supply and demand [6]. This generates a trans-shipment problem with no intermediate nodes, with each warehouse and market connected, and a set of unit costs, c_{ij}, of shipping from warehouse i to market j. There are efficient linear programming solutions to this class of optimisation problem [7]. Miller et al. have previously used transportation methods to detect breast asymmetries [8]. More recently they have been applied to compare histograms [9].

In our application, signature elements can be thought of as warehouses, each containing goods proportional to the intensity of the element. Alternatively, the elements can be thought of as markets, each requiring goods proportional to the intensity. By considering one signature as supplying goods and another signature as demanding goods, we create a transportation problem. A meaningful solution to the problem is facilitated by choosing a suitable set of costs, c_{ij}, to capture the 2-D structure of the signatures. We have used costs based on the 2-D distance between signature elements, taking into account the periodicity of the orientation axis of the signatures. Thus, localised movement in both scale and orientation is favoured over more global movements. In each of the techniques described later the similarity measure is defined as the mean cost of moving a single unit of intensity: the total cost of transportation divided by the number of units (goods) transported.

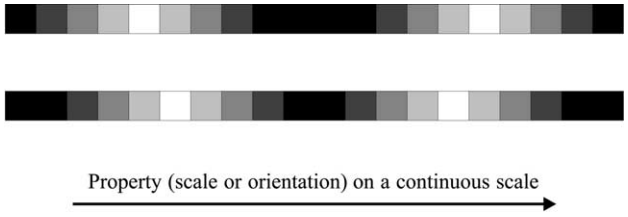

Fig. 2. Comparing similar 1-D signature vectors. The Euclidean distance between them is large, even though the underlying structure they represent is similar.

3. Developing a suitable measure of similarity

Signatures may be obtained from one or more structures embedded in a variable mammographic background. A useful measure of similarity should be able to recognise when similar structures exist in two signatures despite intrinsic variability and regardless of the presence of other background structure. The techniques introduced in this section attempt to address this problem using a transportation framework. Fig. 3 shows two signatures, taken from: (a) a binary line and (b) a binary blob. Visualisations of the solutions to the transport problem are shown for the (c) unnormalised, (d) normalised and (e–h) partial matching techniques discussed below.

3.1. Unnormalised signatures

The simplest method of obtaining a similarity measure involves no pre-processing of the signatures. That is, the 'raw' signatures define the transportation problem. If the sum of intensities in the two signatures is different, we have an unbalanced problem. This is commonly known as

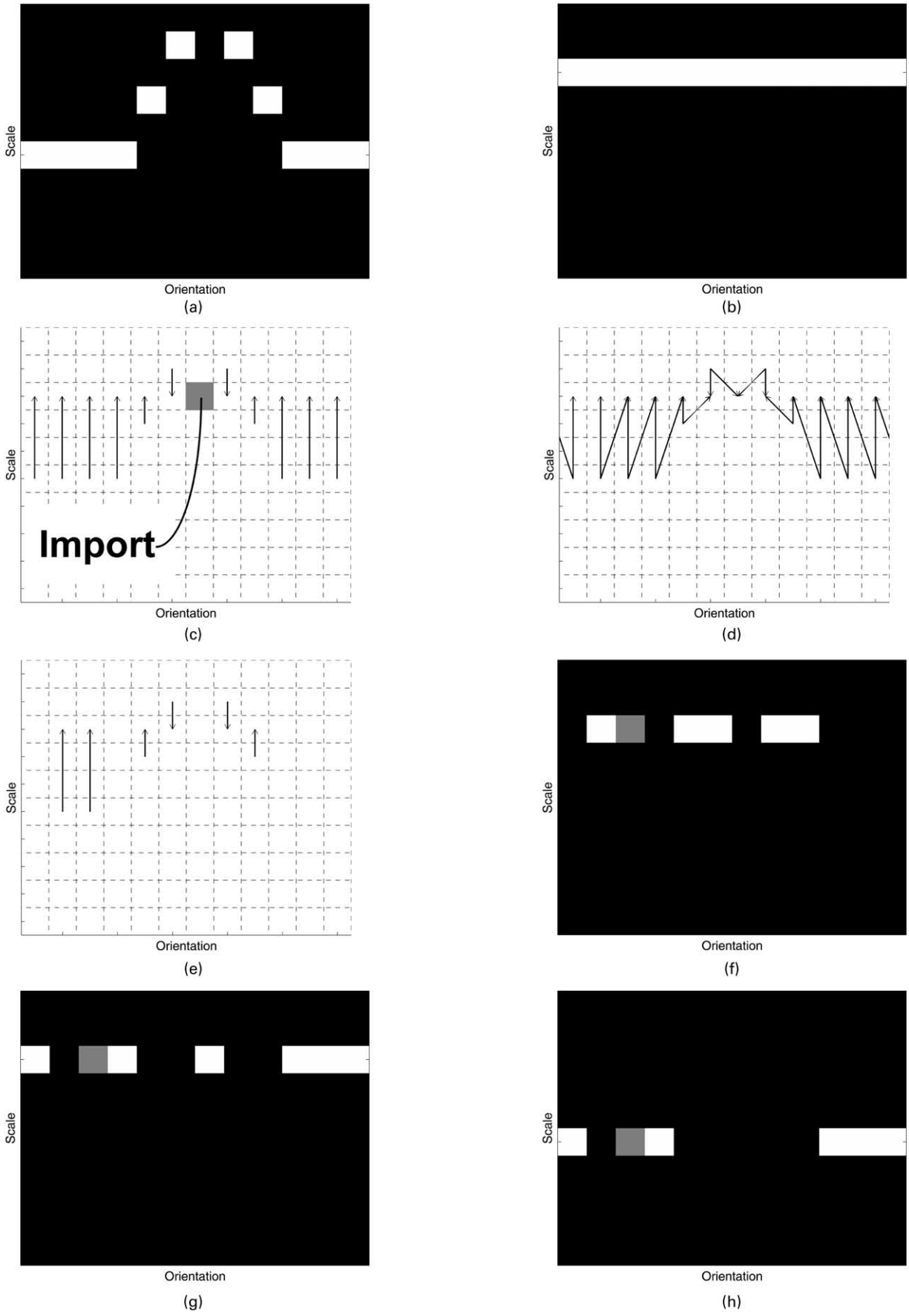

Fig. 3. Transportation between signatures from: (a) a binary line and (b) a binary blob. Transportation using unnormalised signatures is shown in (c) and normalised signatures in (d). (e–h) show an example of partial matching at 50%. Internal movement (e), result of internal movement (f), import (g) and export (h). Using partial matching, some elements have only part of their content transported in the solution, as indicated by the grey elements in (f–h).

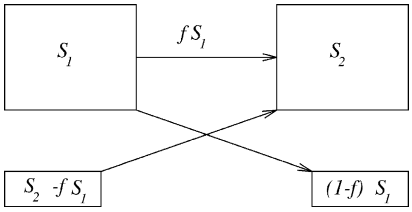

Fig. 4. Partial matching using the transportation problem.

the 'non-standard' transportation problem and is solved by introducing an extra warehouse (or market) to provide (or absorb) the difference. Movement to or from this extra location is free (zero cost). A visualisation of the solution is shown in Fig. 3(c). As the signatures are unbalanced, when transporting from signature (a) to signature (b), the extra units required have been imported.

3.2. Normalised signatures

An alternative approach is to pre-process the signatures to equalise their totals. The simplest way to do this is, for both signatures, to multiply each element in one signature by the total elements in the other signature. Thus a balanced problem is created and a solution exists without the need for an extra location to supply or absorb excess material. Fig. 3(d) shows the solution for matching the two binary signatures. As the signatures are normalised, no external goods are required.

3.3. Partial matching

Our final method is motivated by the observation that, in real applications, it is likely that similar structures will be embedded in different backgrounds, resulting in partial similarity between signatures. This suggests that a fraction of one signature should match the other. Fig. 4 shows schematically how partial matching works. The larger boxes are the signatures and the smaller boxes are a dummy warehouse and market. The first signature has a total supply of S_1 goods and the second signature requires S_2 goods. We choose a specified fraction of the first signature, fS_1, to describe the second signature. This dictates what the values in the dummy warehouse and market should be to create a balanced problem. The inter-signature costs are defined as before. The cost of moving between a dummy and signature location is chosen to be the same as moving to an adjacent 4-connected element within a signature. Varying this value determines the ratio of internal to external movement. Movement between the two dummy locations is prohibited. Fig. 3(e–h) shows the transportation solution at an arbitrary matching fraction of 50%. Five and a half units have been moved 'internally' and the rest have been 'exported' or 'imported'. Some of the signature elements have been

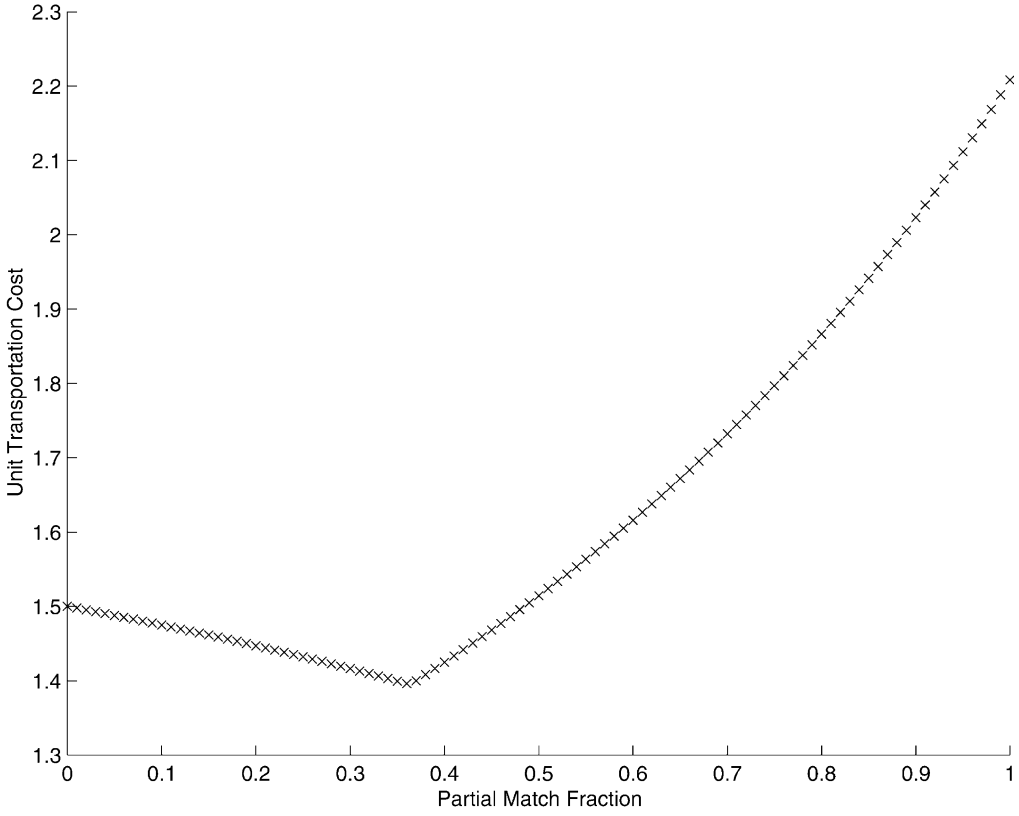

Fig. 5. Unit transportation cost as a function of partial match fraction, f, for the two signatures shown in Fig. 3. The minimum unit transportation cost is 1.396 at a partial match fraction of 0.36.

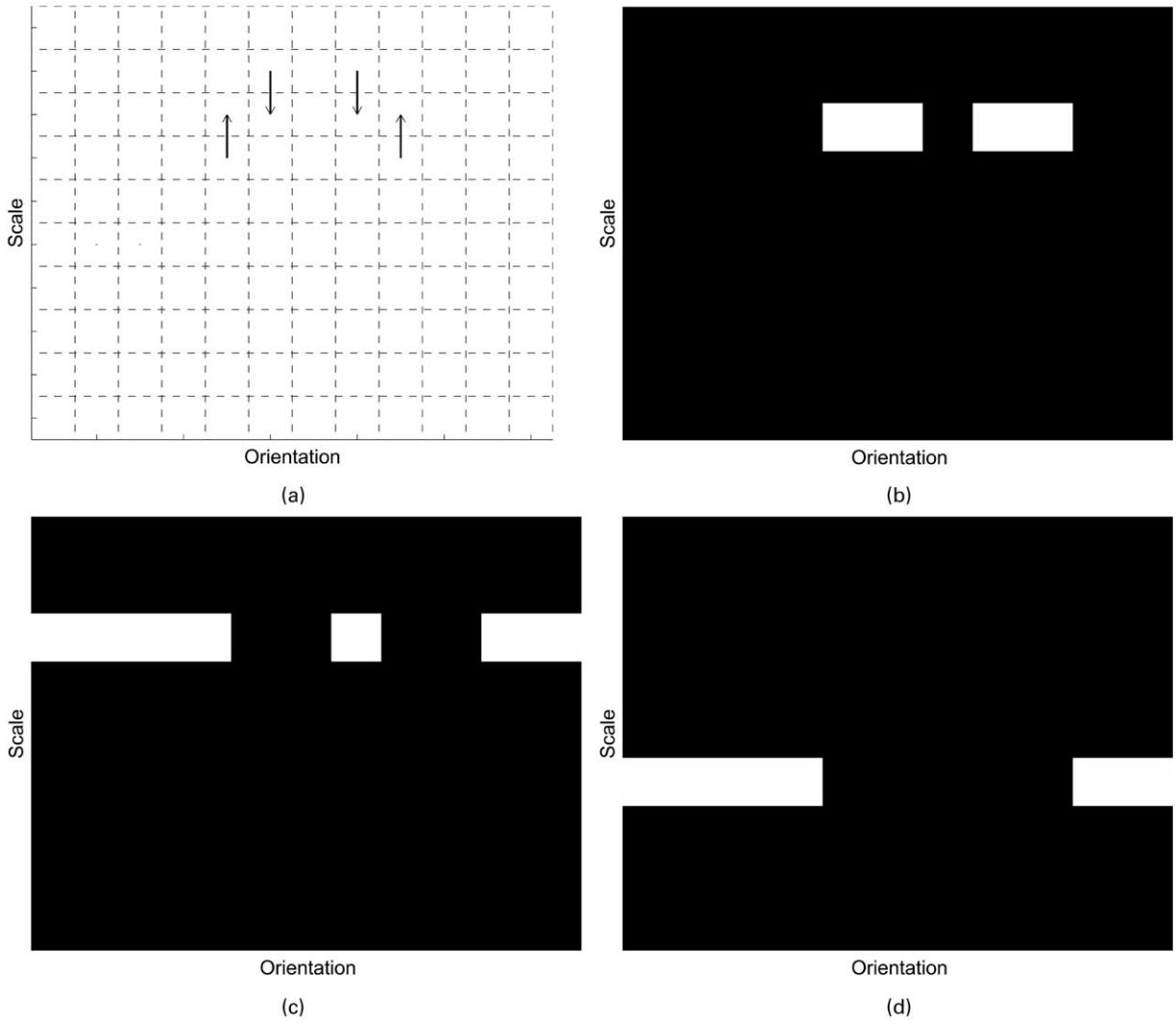

Fig. 6. BPM solution for the two signatures from Fig. 3 showing: (a) internal movements, (b) the result of internal movement, (c) imported material and (d) exported material.

matched successfully by moving units a small distance but, because the matching fraction has been chosen arbitrarily, some units have been moved a long way.

3.4. Best partial matching

We can solve the problem of finding an appropriate value for the partial match fraction f by considering the unit transportation cost as a function of f. This is shown in Fig. 5 for the two signatures from Fig. 3. There is a minimum in the transportation cost at the value of f that results in the best description of one signature in terms of the other. The resulting partial match is shown in Fig. 6. This best partial match (BPM) solution finds the structure common to both signatures, but imports and/or exports the remaining material. We currently use a polynomial fit iterative search to find the BPM fraction at which the minimum cost occurs.

4. Experimental evaluation

In the following experiments, signatures were formed from the set of test images by applying a set of 1-D morphological M filters, centred on every image pixel. Ten scales were used that increased logarithmically and were chosen to encompass the range of structure sizes that occur in mammograms. At each scale, the filter was applied at 12 orientations, separated by 15°.

4.1. Synthetic data

4.1.1. Method

A synthetic image set was constructed from combinations of a Gaussian line, Gaussian blob and fractal-generated background similar to those found in mammograms. Using synthetic data allows the exact definition of ground truth and so produces objective quantitative results. In addition, when comparing images containing the Gaussian line,

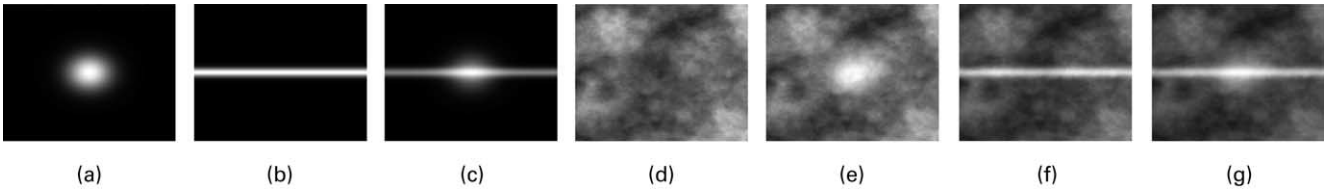

Fig. 7. The synthetic image test set consists of a: (a) blob, (b) line, (c) blob and line, (d) background, (e) blob and background, (f) line and background and (g) blob, line and background.

there is no need to search over orientation as all occurrences of the line are identical. Thus, each signature comparison is faster and more signatures can be examined. Fig. 7 shows the synthetic images used.

Two experiments were performed with the synthetic data. Both experiments involved comparing pairs of images from the test set. For each comparison, 200 pixels were chosen randomly from a structure of interest in one of the images. Similarity distances were then measured between the 200 chosen pixel signatures and their counterparts in the other image using each of the methods described in Section 3. By comparing similarity distances between image pairs that contain the same structure and image pairs that do not, ROC analysis could be performed [11].

The first experiment examined the ability of the different techniques to detect a structure in a signature that was contained in another signature. The Gaussian blob, Fig. 7(a), was compared with each of the other images that contain the blob, i.e. Fig. 7(c), (e) and (g). It was then compared with each of the images that do not contain the blob, i.e. Fig. 7(b), (d) and (f). This was repeated using the Gaussian line, comparing it first with images that contain the line and secondly with images that do not. Ideally we should obtain smaller similarity distances for image pairs that contain similar structure.

The second experiment examined the ability of the different techniques to detect a structure that was common to both signatures when both signatures contain more data than just the structure in question. First, the image consisting of a blob and a line, Fig. 7(c), was compared with the image containing a blob on a fractal background, Fig. 7(e). Thus, the blob was the common structure. Fig. 7(c) was then compared with the image containing a line on a background, Fig. 7(f), where the line was the common structure and finally with the background image, Fig. 7(d) where no common structure existed. This final comparison was repeated to ensure that an equal number of samples were taken from image pairs with common structure and with no common structure.

4.1.2. Results

Fig. 8 summarises the results of the synthetic data experiments described earlier. Receiver operating characteristic (ROC) curves are used to show the ability of the different

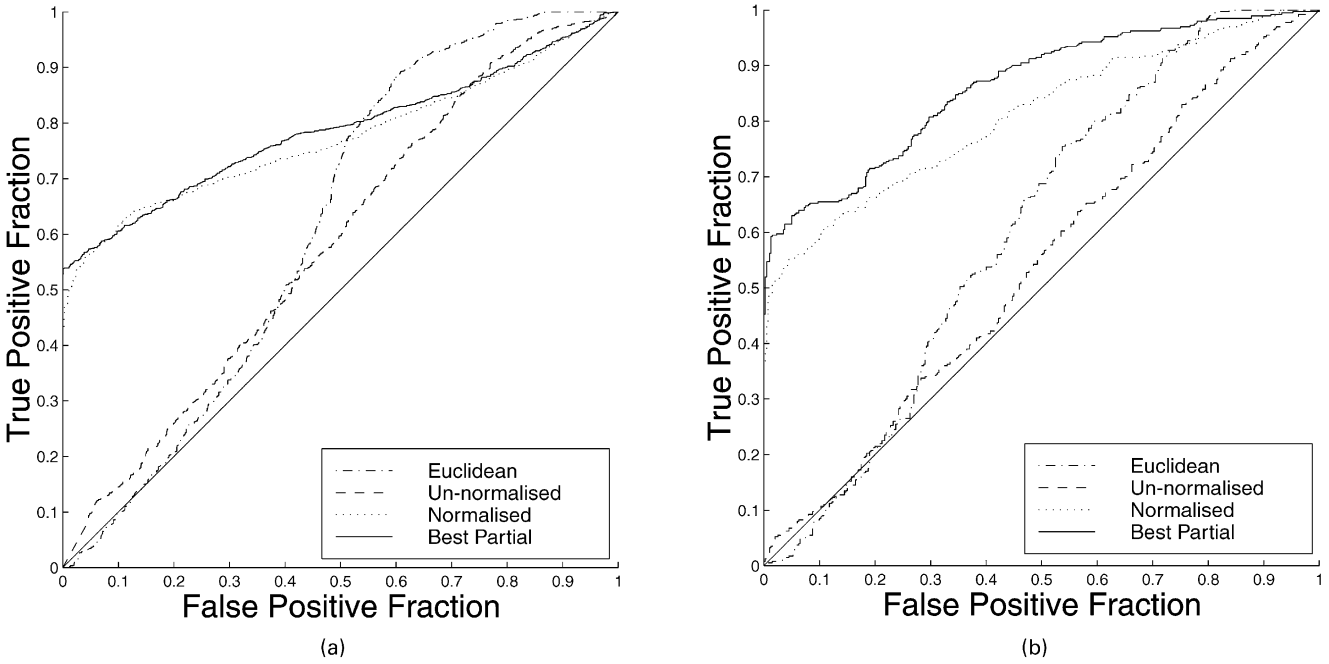

Fig. 8. ROC curves for comparisons between pixel signatures: (a) where one signature is *contained* in the other and (b) where both signatures contain a *common* structure.

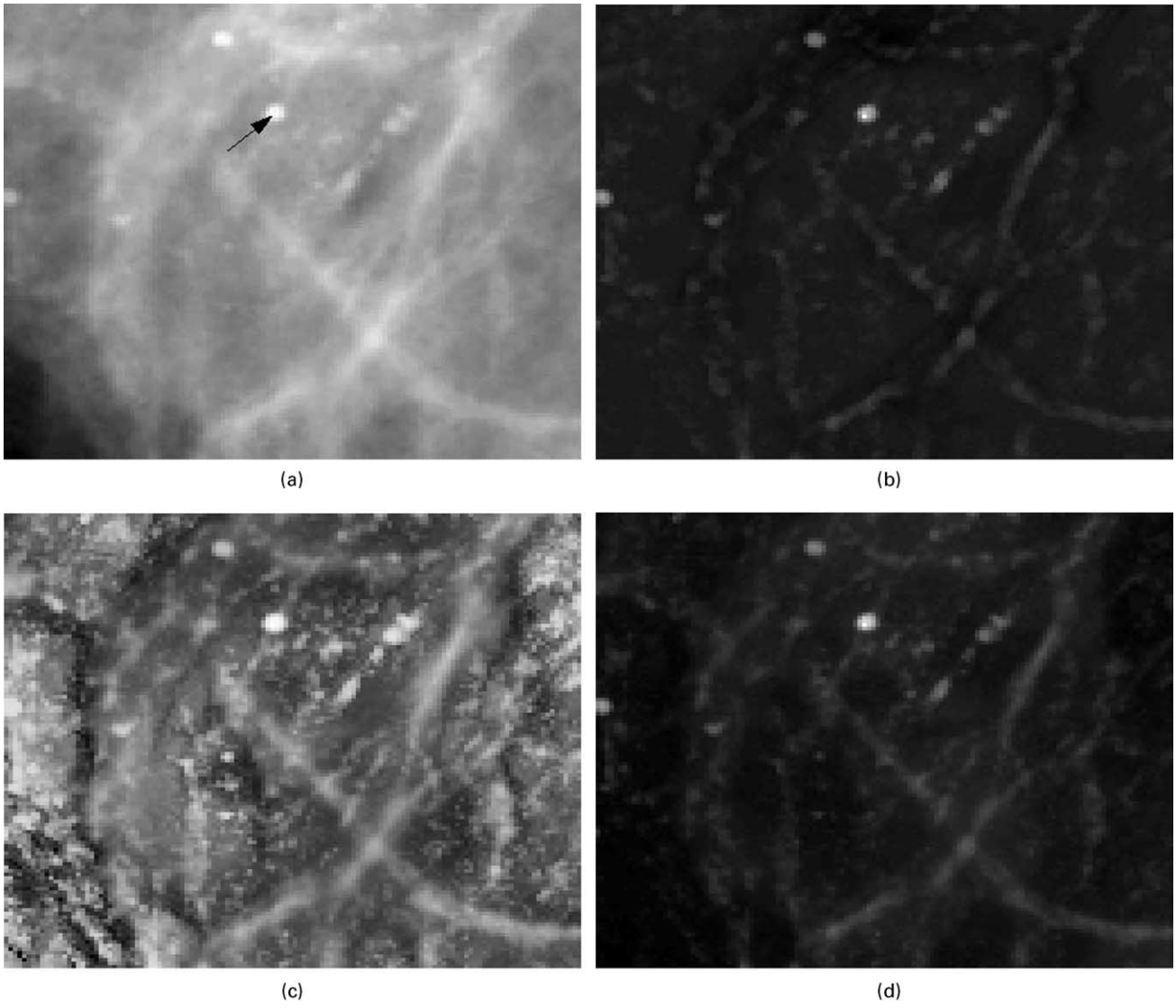

Fig. 9. Similarity images for a pixel signature taken from: (a) a classification using (b) Euclidean, (c) normalised transportation and (d) BPM transportation distances.

measures to discriminate between signature pairs drawn from matching or non-matching structures [11]. Each curve plots the fraction of correct matches against the fraction of false matches as a matching threshold is varied. An ideal distance measure would minimise the area above and to the left of the curve. A curve lying on the main diagonal indicates a random decision process (no discrimination).

It is clear that the normalised and BPM methods generally outperform the unnormalised and Euclidean methods in both the experiments. In Fig. 8(a), there is little difference between the normalised and BPM methods but in Fig. 8(b), the BPM method is clearly superior to all the other methods. This demonstrates the expected superiority of BPM in dealing with common structure. This second experiment is a closer approximation to the clinical applications in which the methods would be used, so these results encourage us to examine their performance with real mammogram data.

4.2. Mammogram data

4.2.1. Method

In order to investigate the performance of the methods in a clinical environment, a region of interest (ROI) was selected from a mammogram (mdb245ls) from the MIAS database [10]. The ROI contains several blob-like structures and several linear structures. Two pixels were chosen, one from a blob-like classification and the other from a linear structure. For each of the chosen pixels, the ‘similarity distance’ between the chosen pixel’s signature and every pixel signature in the ROI was measured using each of the methods described in Section 3. In contrast to the experiments using synthetic data, real structures may occur at any orientation and thus it was necessary to search over all orientations when comparing signatures. Plotting the similarity

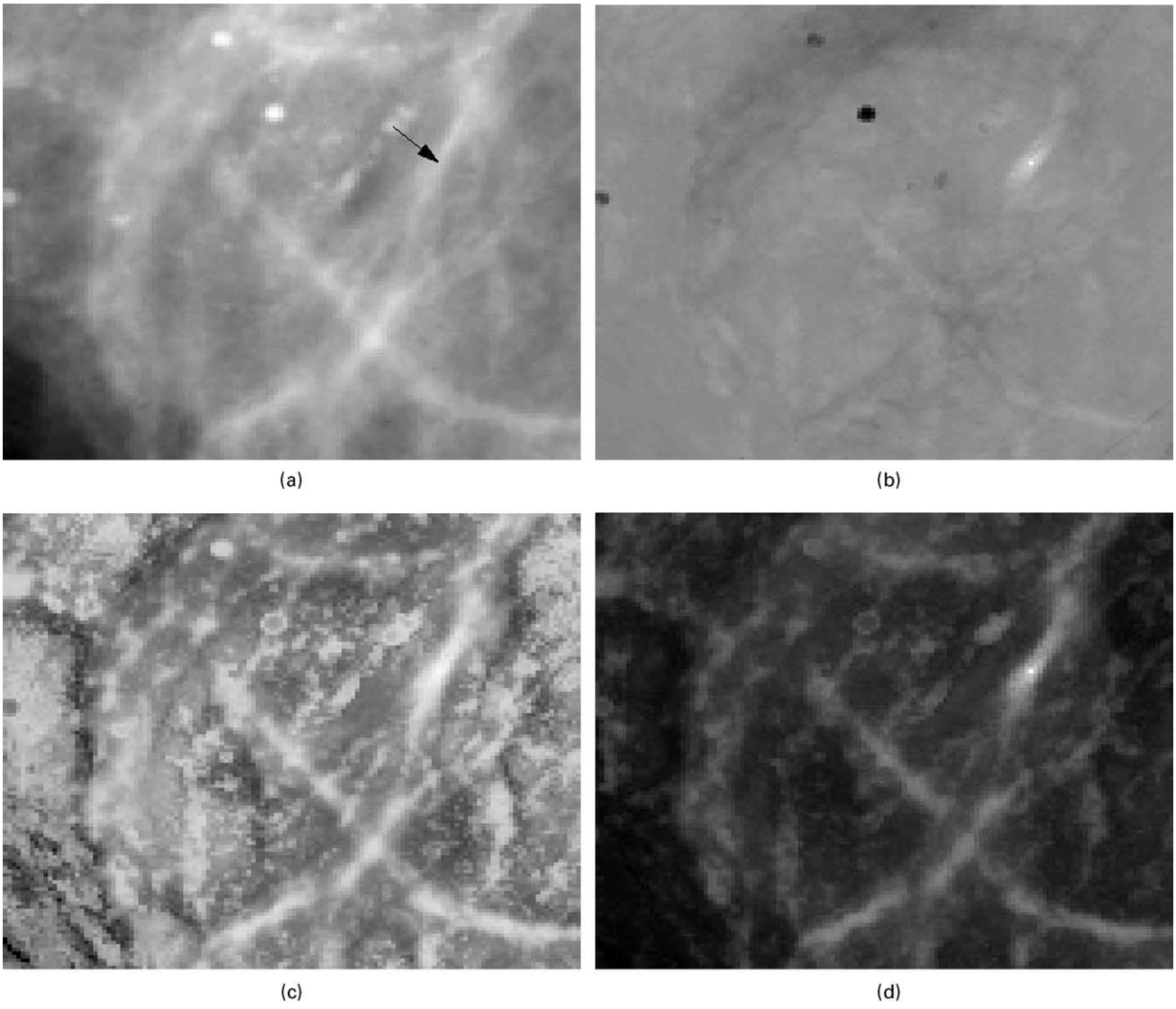

Fig. 10. Similarity images for a pixel signature taken from: (a) a linear structure using (b) Euclidean, (c) normalised transportation and (d) BPM transportation distances.

distance at each pixel forms a similarity image for each method. These images were inverted so that bright regions indicate similar pixels and dark regions pixels that were less similar. The image intensity was scaled between the largest and smallest similarity distances present in the image.

4.2.2. Results

Figs. 9 and 10 show the results of the experiment with real mammogram data described earlier. The results obtained using the unnormalised transportation method were much worse than those for the other methods and are not shown. This inferior performance was to be expected given the results of the experiments with synthetic data.

Fig. 9(b)–(d) show the 'similarity images' generated by comparing each signature with that for a pixel from the blob-like classification indicated in Fig. 9(a). Fig. 10(b)–(d) show the 'similarity images' generated by comparing with a pixel taken from the linear structure indicated in Fig. 10(a).

5. Discussion

The results for the synthetic experiment, shown in Fig. 8, indicate that at high specificities, or low false positive fractions (FPF), the normalised and BPM methods have higher sensitivities, or higher true positive fractions (TPF), than either the unnormalised or Euclidean methods. This means that they will detect matching structures more successfully than the Euclidean method. Fig. 8(a) shows that there is little difference in performance between the normalised and BPM methods when comparing signatures from a given structure with others that contain that structure.

Fig. 8(b) shows, however, that the BPM method is superior when attempting to detect common structure between signatures. Surprisingly, the unnormalised transportation method performs less efficiently than Euclidean distance. We believe this is due to contrast differences across the synthetic image data leading to severely unbalanced transportation problems in the unnormalised case.

From Fig. 9 we observe that the similarity images generated from the mammogram by the Euclidean and BPM methods are remarkably similar. They have both successfully delineated blob-like structures and rejected other material. The signal-to-noise ratio for the BPM result may be slightly better, but it is impossible to tell without knowledge of ground truth that is, by definition, not available for the real mammogram data. The signal-to-noise ratio for the normalised transportation method is clearly worse than that for the other two methods. This is consistent with results for synthetic data shown in Fig. 8 where the normalised transportation method was shown to exhibit lower sensitivity (TPF) at high specificity (low FPF) than the other two methods. The fact that the performance of the Euclidean and BPM methods are similar suggests that the situation is comparable with that in the first synthetic experiment (Fig. 8(a)) because the 'blob' from which the pixel has been selected sits on a fairly uniform background, thus its signature is likely to be contained in those from other blobs.

The results shown in Fig. 10 for the experiment aimed at detecting linear structure in the mammogram suggest that the situation here is more comparable with that in the second synthetic experiment (common structure) and provides evidence for the superiority of the BPM method. The difference between the images generated by the Euclidean and BPM methods is considerably greater than in Fig. 9. In fact, the most striking feature of the results is that the Euclidean method has clearly rejected the blob-like structures whilst remaining reasonably indifferent to the presence of linear structure. Again, the normalised transportation method gives a significantly lower signal-to-noise ratio than the other two methods though the linear structures have been detected with reasonable sensitivity. Most importantly, the BPM method has successfully detected linear structures and suppressed other structures and background. These results indicate that our approach measures signature similarity in a practically useful way.

The major drawback with the approach is that calculation of the BPM distance measure is computationally expensive; it takes nearly 2 days on a Pentium III processor to calculate a set of similarity images, such as those shown in Figs. 9 and 10. We have recently shown that BPM distance can be successfully approximated by learning a transformation from the signature space into a new space. In this new space, Euclidean distance approximates BPM distance [12]. Once this transformation has been learnt 'off-line', images such as those in Figs. 9 and 10 take approximately a quarter of a second to generate, allowing the BPM metric to be used at run-time.

6. Conclusions

The work presented in this paper significantly extends previous work on structure detection and classification using scale-orientation pixel signatures [3]. A significant drawback with signatures is their unsatisfactory metric behaviour when treated as vectors and subjected to statistical analysis. We have developed a sophisticated and novel method of measuring signature similarity that is based on the transportation algorithm [6]. By investigating its use with synthetic data, we have shown that this best partial match measure detects the presence of similar structure in signatures in the presence of intrinsic variability and potentially confounding background structure. Application to real mammogram data has shown that the measure is effective in detecting similarities between both blob-like and linear structures. We are currently using these results as a basis for developing a comprehensive and efficient scheme for creating statistical models of local appearance for use in medical image analysis in general and computer-aided mammography in particular.

Acknowledgements

We would like to thank Reyer Zwiggelaar who gave helpful comments and the fractal background generation code; he is currently at the University of East Anglia. Anthony Holmes and Chris Rose were funded by EPSRC studentships.

References

[1] I.W. Hutt, S.M. Astley, C.R.M. Boggis, Prompting as an Aid to Diagnosis in Mammography, Digital Mammography, Elsevier, Amsterdam, 1994 pp. 389–403.
[2] D.J. Marchette, R.A. Lorey, C.E. Priebe, An analysis of local feature extraction in digital mammography, Pattern Recognition 30 (9) (1997) 1547–1554.
[3] R. Zwiggelaar, T.C. Parr, J.E. Schuum, I.W. Hutt, S.M. Astley, C.J. Taylor, C.R.M. Boggis, Model-based detection of spiculated lesions in mammograms, Medical Image Analysis 3 (1) (1999) 39–62.
[4] J.A. Bangham, T.G. Campbell, R.V. Alridge, Multiscale median and morphological filters for 2D pattern recognition, Signal Processing 38 (1994) 387–415.
[5] R. Harvey, A. Bosson, J.A. Bangham, The robustness of some scale-spaces, British Machine Vision Conference, BMVA Press, 1997, pp. 11–20.
[6] F.L. Hitchcock, The distribution of a product from several sources to numerous localities, J. Math. Phys. 20 (1941) 224–230.
[7] A. Ravindran, D.T. Phillips, J.J. Solberg, Operations Research: Principles and Practice, Wiley, New York, 1987.
[8] P. Miller, S. Astley, Automated detection of breast asymmetries, British Machine Vision Conference, BMVA Press, 1993, pp. 519–528.
[9] Y. Rubner, C. Tomasi, L.J. Guibas, A metric for distributions with applications to image databases, Proceedings of the Sixth International Conference on Computer Vision, IEEE, 1998, pp. 59–66.
[10] J. Suckling, J. Parker, D. Dance, S. Astley, I. Hutt, C. Boggis, I. Ricketts, E. Stamatakis, N. Cerneaz, S. Kok, P. Taylor, D. Betal, J. Savage, The mammographic images analysis society digital

mammogram database, Excerpta Medica. International Congress Series 1069 (1994) mias@sv1smbmanacuk.

[11] C.E. Metz, ROC methodology in radiologic imaging, Investigative Radiology 21 (1986) 720–733.

[12] A.S. Holmes, C.J. Taylor, Transforming pixel signatures into an improved metric space, British Machine Vision Conference, BMVA Press, 2000, pp. 805–814.